

Numerical Model of White Dwarf's Magnetic Field Evolution

Shu Zhang

Supervisor: Andrew Cumming

(McGill University)

(Dated: April 25, 2024)

White dwarfs, the remnant of low-mass stars' death, are compact small stellar objects, that slowly dissipate their thermal energy. They last for over 10 billion years before completely crystallizing. They are also commonly observed to be strongly magnetized. The origin of this strong magnetic field has always been mysterious. Several studies reveal a possible explanation: white dwarf's core crystallization imposes compositional convection, which, further combined with stellar rotation, could drive a dynamo, in analogy to Earth's core dynamo. In the past, this process was believed to be insufficient to support the large intensity of the observed magnetic field. A recent study[1], in which the author combines mixing-length theory with scalings from magnetorotational convection, shows possible higher convection velocity, sufficiently supporting observation with an estimation of field strength $\sim 10^6 - 10^8$ G. However, this is the strength of the initial magnetic field which starts only in the convection zone. After several billion years, the star cools down, and such a field diffuses and reveals itself at the star's surface. A loss in magnetic energy during the diffusion will reduce the field intensity. With numerical calculation, we found that for an initial field size of $\sim 0.2R_{WD} - 0.8R_{WD}$, the intensity of the surface field is $\sim 10^{-4} - 10^{-1}$ of the original. This result is consistent with observations, making the core-convection mechanism a stronger argument.

I. WHITE DWARF MAGNETIC FIELD ORIGIN

In a living star, nuclear fission energy supports against gravitational energy from collapsing inward. This is hydrostatic equilibrium. Eventually, after billions of years, such nuclear fuel will exhaust, and gravity will dominate, collapsing the object into something more compact. This marks the death of a star. The mass of the star will determine its fate in the next stage. While massive ones collapse into black holes and neutron stars, the ones close to one solar mass will die less dramatically and turn into white dwarfs. White dwarfs are hot but not luminous, due to their small size. They have a very long lifespan, in the order of 10 billion years. They are essentially remnants of low-mass stars' core, composed of carbon and oxygen.

Many white dwarfs are observed to have a strong magnetic field, $10^4 G \sim 10^9 G$ (million times of Earth). The origin of this field is unclear, one possible mechanism is that crystallization of the star's core drives compositional convection, as oxygen tends to be pulled into the crystal core and carbon tends to remain in the liquid. Then this convection combined with the star's rotation, can drive a dynamo, just like Earth's core dynamo.

While the real convection behaviour must be more chaotic, what is really important is the size of the convection zone and the typical convective velocity. The size of initial convection zone determines the size of the initial magnetic field B_0 . This is a quantity that remains unclear, ideas have been proposed to estimate it to be around $0.5R_{WD} \sim 0.8R_{WD}$ [2]. In the past, it is believed that the convective velocity is not sufficient to produce a strong field ($10^{-6} \sim 10^{-5} cm/s$ corresponding to 100 G). But recently, we found it is possible, for only about one million years after the birth of a white dwarf, for

$10^2 \sim 10^3 cm/s$ (corresponding to a field strength of $10^6 G$ to $10^8 G$) convective velocity to exist, and therefore to generate a field that is strong enough to explain observations. In Fig. 1, the blue line shows the proposed field strength but right now it doesn't make sense as it misses all the data points. That's why we need to calculate the magnitude of field at the surface of the white dwarf instead of the initial field strength.

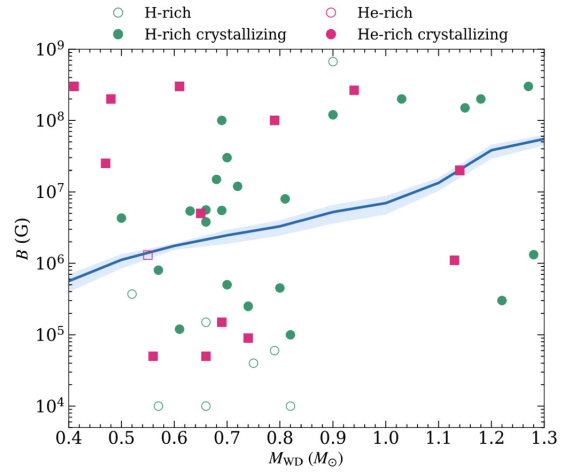


FIG. 1. A figure showing the observed field strength for sample white dwarfs, and the proposed field strength generated by strong convection, made by Matias[1]. Unfortunately, the field line perfectly avoids all the observation data. But this shows only the intensity of the original field which starts in the convection zone. The field will diffuse and be revealed at surface with reduced strength. As explained in Sec.V, the line will be brought down to only 0.05 of the original value due to field diffusion. In that case, the line will pass through the majority of points at the bottom.

II. FIELD PROPAGATION

During the process when the field, initially started only in the convection zone, diffuses to the surface, it loses a significant amount of strength. Extending the modelling forward in time will reveal how the magnetic fields evolve and diffuse as the star cools. To track the change of magnetic field in time, we begin with the Maxwell's equations (in cgs unit):

$$\frac{1}{c} \frac{\partial B}{\partial t} = -\nabla \times E,$$

$$\frac{4\pi}{c} J = \nabla \times B,$$

substituting with Ohm's law

$$J = E\sigma(t),$$

then, rewrite conductivity σ in terms of diffusivity $\eta = c^2/4\pi\sigma$ we reach the induction equation, which tells how the field evolves due to the field itself

$$\frac{\partial \vec{B}}{\partial t} = -\vec{\nabla} \times (\eta \vec{\nabla} \times \vec{B}), \quad (1)$$

where $\eta = c^2/4\pi\sigma$ is the magnetic diffusivity and σ is the electrical conductivity. From this equation, with mathematical operations, we can find the eigenmodes for a liquid white dwarf, following the work of Andrew Cumming (2002)[3]. With assumption of an axisymmetric poloidal magnetic field, where \vec{B} could be decomposed into only radial r and θ direction, $\vec{B} = B_r \hat{e}_r + B_\theta \hat{e}_\theta$ and the fact field could be written in form of vector potential $\vec{B} = \nabla \times \vec{A}$ where $\vec{A} = A_\phi(r, \theta, t) \hat{e}_\phi$, we could use the identity $\nabla \times (\hat{e}_\phi / r \sin\theta)$ to get the relation:

$$B = \frac{\hat{e}_\phi}{r \sin\theta} \times \nabla(r A_\phi \sin\theta)$$

Further separating A_ϕ into radial and angular components:

$$A_\phi(r, \theta, t) = \sum_l \frac{R_l(r, t)}{r} P_l^1(\cos\theta).$$

The magnetic field could finally be expanded into the following equations:

$$B_r = \sum_l \frac{l(l+1)}{r^2} R_l(r, t) P_l(\cos\theta). \quad (2)$$

Substituting this equation for field radial strength into the induction Eqn. 1 to get

$$\frac{\partial R_l}{\partial t} = \eta(r, t) \left[\frac{\partial^2 R_l}{\partial r^2} - \frac{l(l+1)R_l}{r^2} \right], \quad (3)$$

which will be able to track the evolution of the magnetic field with given diffusivity profile $\eta(r, t)$. Two boundary

conditions must be applied. First, the magnetic field must be finite at the center of the star. This requires when $r \rightarrow 0$:

$$\frac{\partial R_l}{\partial r} - \frac{l+1}{r} R_l \rightarrow 0. \quad (4)$$

Second, the field at the stellar surface must approach continuously the field in the vacuum, which demands when $r \rightarrow R_{WD}$

$$\frac{\partial R_l}{\partial r} + \frac{l}{r} R_l \rightarrow 0. \quad (5)$$

Since Eqn. 3 is an equation hardly solvable analytically (only solvable for the special case where diffusivity η is constant, in fact, that is the key to checking whether the algorithm is functioning properly mentioned in Sec.IV), numerical methods will be necessary.

III. NUMERICAL CALCULATION

To solve the equation numerically, it needs to be transformed by taking finite differentiation. With Talyor expansion locally at a small difference Δx , any function could be written in:

$$f(x + \Delta x) \approx f(x) + \Delta x \frac{df}{dx} + \frac{(\Delta x)^2}{2} \frac{d^2 f}{dx^2} + \dots$$

Implying both forward $R_l(r + \Delta r)$ and backward $R_l(r - \Delta r)$, a second order differential equation could be represented by:

$$\frac{\partial^2 R_l}{\partial r^2} = \frac{R_{i-1} - 2R_i + R_{i+1}}{(\Delta r)^2} + \mathcal{O}(\Delta r)^2$$

where subscript i denotes the points on a finite grid. And easily, the time differential is

$$\frac{\partial R_l}{\partial t} = \frac{R_i^{n+1} - R_i^n}{\Delta t}. \quad (6)$$

A. Need for Crank–Nicolson method

It is important to keep the error within the tolerance, thus we demand low error in updating the time steps. However, the evolution of white dwarf field happens in the timescale of billions of years, it is irrational to take tiny time steps in the scale of seconds. Explicit methods require small time steps Δt to achieve high accuracy, so we use implicit methods instead.

Hence, the Crank–Nicolson method is introduced.

$$\begin{aligned} \frac{R_i^{n+1} - R_i^n}{\Delta t} &= \frac{1}{2} \left[\frac{R_{i-1}^{n+1} - 2R_i^{n+1} + R_{i+1}^{n+1}}{(\Delta r)^2} \right] \\ &+ \frac{1}{2} \left[\frac{R_{i-1}^n - 2R_i^n + R_{i+1}^n}{(\Delta r)^2} \right] \end{aligned} \quad (7)$$

Crank–Nicolson method is a second-order method in time, thus high accuracy. And it is tested to be unconditionally stable for solving diffusion equations[4], which fits our need. Even when taking large time steps and small grid spacing, it will remain relatively stable.

B. Matrix Operation in Python

If to substitute both Eqn. 6 and Eqn. 7 into the diffusion equation[3], we can rewrite the equation in the form of matrix operation

$$\mathbf{M} \cdot R^{n+1} = \mathbf{N} \cdot R^n \quad (8)$$

$$\mathbf{M} = \begin{bmatrix} \ddots & & & \\ -\alpha_i/2 & 1 + \alpha_i + \beta_i/2 & -\alpha_i/2 & \\ & & \ddots & \\ \alpha_i/2 & 1 - \alpha_i - \beta_i/2 & \alpha_i/2 & \\ & & & \ddots \end{bmatrix}$$

$$\mathbf{N} = \begin{bmatrix} \ddots & & & \\ \alpha_i/2 & 1 - \alpha_i - \beta_i/2 & \alpha_i/2 & \\ & & \ddots & \\ & & & \ddots \end{bmatrix} \quad (9)$$

where \mathbf{M} and \mathbf{N} are tridiagonal matrices, with $\alpha_i = \eta_i(r_i, t_n)\Delta t/\Delta r^2$ and $\beta_i = \alpha_i l(l+1)/r^2$. The boundary condition at the centre of the star demands that

$$\mathbf{M}_{00} = 1 + \alpha_0 \left(1 + \frac{(l+1)\Delta r}{r_0} \right) + \frac{\beta_0}{2},$$

$$\mathbf{N}_{00} = 1 - \alpha_0 \left(1 + \frac{(l+1)\Delta r}{r_0} \right) - \frac{\beta_0}{2},$$

and

$$\mathbf{M}_{01} = -\alpha_0,$$

$$\mathbf{N}_{01} = \alpha_0.$$

The boundary condition at the surface of the star suggests:

$$\mathbf{M}_{i,i} = 1 + \alpha_i \left(1 + \frac{l\Delta r}{r_i} \right) + \frac{\beta_i}{2},$$

$$\mathbf{N}_{i,i} = 1 - \alpha_i \left(1 + \frac{l\Delta r}{r_i} \right) - \frac{\beta_i}{2},$$

and

$$\mathbf{M}_{i,i-1} = -\alpha_i,$$

$$\mathbf{N}_{i,i-1} = \alpha_i.$$

where a grid size of i .

Transforming the equations into matrix form makes it more accessible in Python. Solving for $R^{n+1} = \mathbf{M}^{-1}\mathbf{N} \cdot R^n$ with given $\eta_i(r_i, t_n)$ will produce radial function R^{n+1} for the next time step. Iterating this calculation will trace the evolution of the field. This is the foundation of this article, calculations will depend on the $\eta(r, t)$. In order to produce accurate diffusivity profiles, a clear understanding of the white dwarf's internal structure and its dynamics is necessary, for which one should refer to the work of Matias[1]. It is also possible to modify the diffusivity profile to further investigate the behaviour of enhanced diffusivity (discussion in Sec. VIA). All of which are easily achievable in Python. Please refer to the appendix for details on the code.

IV. ANALYTICAL SOLUTION CHECK

Because of the difference between solid and liquid lattice structures, the conductivity is largely increased when material is crystallized. This is why diffusivity profile changes drastically over time. Now consider the special case, following section 2 of Wendell's work[5], where in Eqn. 3, the diffusivity remains constant. Then there is a solution that decays exponentially with time τ_{ln}

$$R_l(r, t) = \sum_n C_{ln} X_{ln} \exp\left(-\frac{t}{\tau}\right)$$

where C_{ln} is constant determined by mode n , and X_{ln} are eigenfunctions from

$$\frac{d^2 X_{ln}}{dr^2} - \frac{l(l+1)}{r^2} X_{ln} + \frac{1}{\eta(r)\tau_{ln}} X_{ln} = 0.$$

It turns out the eigen solutions are $X_{ln} = \rho j_l(\rho)$ where the spherical Bessel function of the first kind:

$$j_l(\rho) = (-1)^l \rho^l \left(\frac{d}{\rho d\rho} \right)^l \frac{\sin(\rho)}{\rho}$$

and

$$\rho = r \sqrt{\frac{4\pi\sigma(R_{WD})^2}{c^2\tau_{ln}}}.$$

Solving X_{ln} at boundaries (satisfying Eqn. 4 and Eqn. 5) leads to $j_{l-1}(\rho_1) = 0$, where ρ_1 is the value at the surface of star, eigenvalues of the solution to the equation. For the situation we consider, dipole field ($l = 1$), the values are $\rho_1 = n\pi$ for $n = \mathbb{Z}^+$. Thus, the decay times are

$$\tau_{ln} = \frac{4\pi\sigma(R_{WD})^2}{c^2 n^2 \pi^2} \quad (10)$$

Therefore, by feeding a constant diffusivity profile into the algorithm, we expect the function $\rho j_l(\rho)$ to exponentially decay with a characteristic time scale of τ_{ln} . This could verify whether the code is behaving properly or not. As shown in Fig. 2, by examining the difference between initial $X_{ln}(t = 0)$ and $X_{ln}(t) \exp(-t/\tau)$, we verify that the Python code behaves as expected, and the error remains in the scale of 10^{-4} .

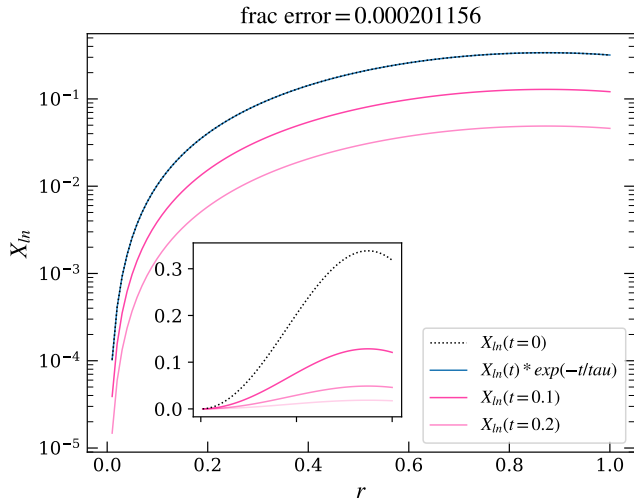


FIG. 2. The difference between $X_{ln}(t) * \exp(-t/\tau)$ and $X_{ln}(t = 0)$ is shown as fractional error at the top. X_{ln} is the spherical Bessel function $j_p(r)$. The samples are chosen at linearly spaced time points, $t = 0.1, 0.2, 0.3$. The subplot shows the function in linear scale. Since, in the main plot, the y-axis is in log scale, the fact that functions are separated evenly reveals that the value of $X_{ln}(t)$ decays exponentially, as expected. The fact that $X_{ln}(t) * \exp(-t/\tau)$ and $X_{ln}(t = 0)$ overlay indicates the decay time scale is $-1/\tau$.

V. SIMULATION RESULTS

For this entire article, we consider $l = 1$, which corresponds to a dipole magnetic field. Three different models of white dwarfs are investigated. They have different masses of $0.5M_\odot$, $0.7M_\odot$, and $0.9M_\odot$ respectively. Since the size of the initial field is unknown, while Ginzburg[2] proposes a size range from $0.5R_{WD}$ to $0.8R_{WD}$, we explore a wider range of possible sizes from $0.2R_{WD}$ to $0.8R_{WD}$. We assume that initial field is uniform with constant field strength B_0 . The time range is from t_0 , the time that core crystallization starts, to t_f , roughly about 10 Gyr s, when crystallization completes, where the entire white dwarf is solid. We focus on the surface field strength in ratio to initial internal field strength B_{surf}/B_0 after the white dwarfs are mostly crystalized, where the field stabilized.

A. Magnetic Field "Breakthrough"

As shown in Fig. 3, if the size of the initial field is too small $\sim 0.2R_{WD}$, it will not make it to the surface with significant strength (only $10^{-6}B_0$). Most of the magnetic energy is trapped inside the white dwarf because the core freezes and grows faster than the field could ever propagate to the surface. The field is frozen in. When the size of the original field reaches $\sim 0.5R_{WD}$, the field will diffuse quickly and present at the surface after $\sim 7 \text{ Gyr}$ with a strength of $10^{-2}B_0$. It is only then, that the field

is travelling faster enough to get out to the surface before core crystallization halts the diffusion. This would verify Ginzburg's claim that the size of initial convection zone is around $0.5R_{WD} \sim 0.8R_{WD}$. Anything smaller will not let the magnetic field show significantly at the surface of the star. However, situations will be slightly different if to consider enhanced diffusivity in the convection zone, which is discussed in Sec. VI A.

B. Deduced Field Strength at Surface

As shown in Fig. 3, for initial field size of $0.5R_{WD} \sim 0.8R_{WD}$, the surface field strength will stabilize at $0.01B_0 \sim 0.1B_0$. This would explain why previously in Fig. 1, the theoretical values of field strength do not match with an observation well. This is because when an internally generated magnetic field propagates to the surface the strength reduces to only $0.1 \sim 0.01$ of the original values. Thus what should happen is that the blue line in Fig. 1 drops to start with roughly $\sim 10^5 G$, crossing most of the data points at the bottom half of the graph. This would allow us to conclude, for now, that convection-driven dynamo is a possible and probable mechanism responsible for producing many of the observed magnetic white dwarfs.

VI. FUTURE IMPROVEMENT

It is worth mentioning that the diffusivity profile $\eta(r, t)$ is mainly dependent on the internal composition of white dwarfs. But real fluid behaviour should have more complexity. Some of them are chaotic, and hardly to be traceable. But on a large scale, some fluid behaviour, that we could predict, would change the diffusivity dramatically. Being able to encounter these factors in the calculation will effectively be the future goal of this research. The immediate idea that is already under development, is enhanced diffusivity in the convection zone.

A. Unresolved Enhanced Diffusivity

After the strong convection happens to produce the initial field, the convection will not just vanish. Convection still happens, but not sufficient enough to produce any strength field. As the core still grows in size, the convection zone size changes over time. Such insufficient convection will increase the diffusivity in the region due to turbulent diffusion, capable of transporting magnetic energy at a faster rate. However, it has been extremely difficult to develop a concrete and fully functional model that can be applied to such diffusion behaviour. Thus we have to approximate this effect by assuming a constant boost factor k , which, according to the characteristic mixing length of the fluid, we predict to be a wide range of $5 \sim 1000$.

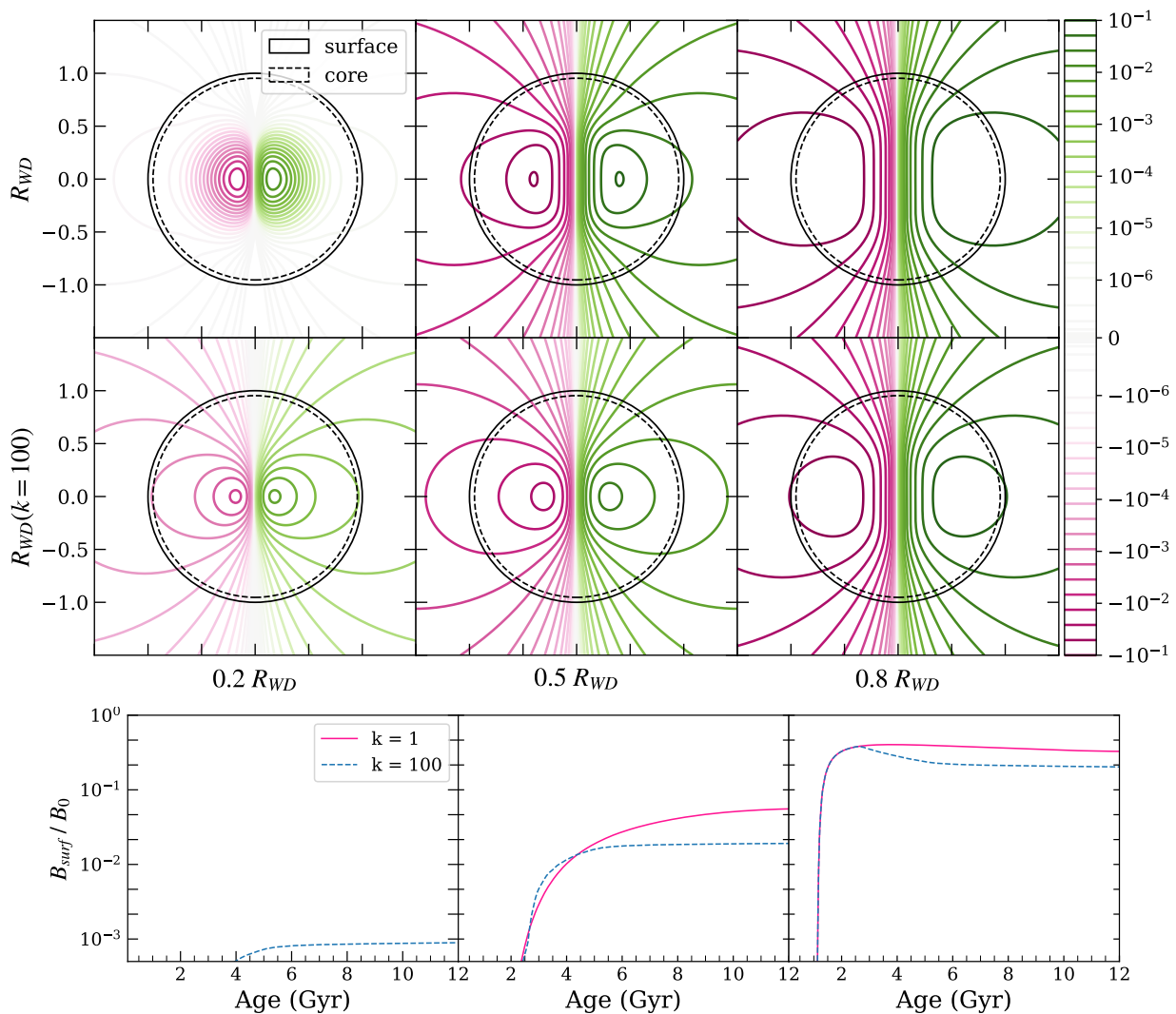


FIG. 3. Simulation of a $0.9M_{\odot}$ white dwarf model. The first two rows show the field line of a dipole configuration ($l = 1$), at age $t_f = 12.6$ Gyr. The first row shows results without enhanced diffusivity in the convection zone, while the second shows results with a boost factor $k = 100$. The last row presents the strength of the field at surface in the ratio to the initial field strength B_{surf}/B_0 , with $k = 1$ indicating results without enhanced diffusivity. The columns indicate different sizes of initial field. As shown, for $0.2R_{WD}$, enhanced diffusivity helps field the propagate to surface, while for $0.8R_{WD}$, enhanced diffusivity acts to decrease surface field strength. The value B_{surf} here is the maximum quantity of radial field strength in Eqn. 2. The field line plotted here is the quantity of $rA_{\phi}\sin(\theta)$.

As shown in Fig. 3, the enhanced diffusivity will allow more magnetic energy to travel to the surface before the crystallization halts the diffusion. Also, the field will show at the surface earlier. For $k = 100$, the resulting field strength at the surface for $\sim 0.2R_{WD}$ is significantly increased (about 500 times strength than unboosted diffusivity). In fact, as shown in Fig. 4, this effect is accessible for initial field size ranging from $0.1R_{WD}$ to $0.3R_{WD}$.

However, the enhanced diffusion speed comes at the cost of increased magnetic energy dissipation. When the initial field size is larger than $0.3R_{WD}$, the effect switches from a boost of surface field strength to a decrease in strength. Thus, according to the observation, we estimate this factor k will not likely be larger than 100.

VII. CONCLUSION

We study the evolution of a white dwarf's magnetic field by solving the induction equation numerically, which simulates the propagation of the magnetic field. We verify that a core-convection-driven dynamo is likely to be the mechanism that explains the origin of a white dwarf's magnetic field. About one million years after core crystallization happens, a strong magnetic field, about $\sim 10^7 G$, is produced by convection. This internal field propagates to the surface of the white dwarf after about ~ 10 Gyr, with a reduced strength of ~ 0.05 of the original field. This result matches the data of many observed magnetic white dwarfs. Additionally, we find that the diffusivity in

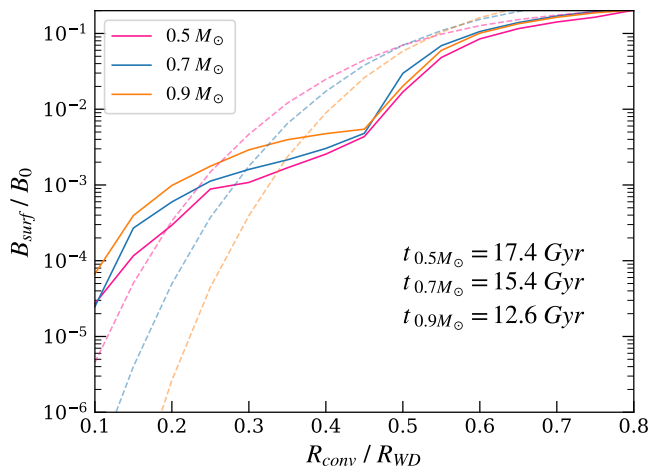


FIG. 4. This graph shows the effect of enhanced diffusivity for white dwarfs with different masses. The t_f at the corner indicates the ages of 3 different models. Smaller white dwarfs take longer to be fully crystalized as they lose thermal energy at a slower rate. Dashed lines in the background represent results without enhanced diffusivity, while solid lines are results with boost factor $k = 100$. As shown, the effect of enhanced diffusivity is stronger for larger white dwarfs.

the convection zone is likely to be boosted due to turbulent diffusion. If that is true, the possibility of an initial magnetic field with size from $\sim 0.1R_{WD}$ to $\sim 0.3R_{WD}$ is largely increased.

ACKNOWLEDGMENTS

This is a project in connection with Matias Castro Tapia's project on modelling the dynamic of white dwarfs' internal structure[1]. He and my supervisor Andrew Cumming lectured me on how the composition of a white dwarf affects the diffusivity profile. It is also Matias' work to calculate the diffusivity profile according to our white dwarf model.

Appendix A: Python code

All the calculations and simulations are easily reproducible. Please refer to the code posted to my GitHub account. The comments and instructions are also included[6].

-
- [1] J. R. Fuentes, M. Castro-Tapia, and A. Cumming, A short intense dynamo at the onset of crystallization in white dwarfs, *The Astrophysical Journal Letters* **964**, L15 (2024).
 - [2] D. Blatman and S. Ginzburg, Magnetic field breakout from white dwarf crystallization dynamos, *Monthly Notices of the Royal Astronomical Society* **528**, 3153–3162 (2024).
 - [3] A. Cumming, Magnetic field evolution in accreting white dwarfs, *Monthly Notices of the Royal Astronomical Society* **333**, 589–602 (2002).
 - [4] J. Liu and Y. Hao, enCrank-Nicolson method for solving uncertain heat equation, *Soft comput* **26**, 937 (2022).
 - [5] C. E. Wendell, H. M. van Horn, and D. Sargent, Magnetic Field Evolution in White Dwarfs, *Astrophys. J.* **313**, 284 (1987).
 - [6] S. Zhang, white dwarf research.